

## Vibrations of the Interstitial Oxygen Pairs in Silicon

M. Pesola,<sup>1</sup> J. von Boehm,<sup>2</sup> and R. M. Nieminen<sup>1</sup>

<sup>1</sup>Laboratory of Physics, Helsinki University of Technology, P.O. Box 1100, FIN-02015 HUT, Finland

<sup>2</sup>LTAM, Helsinki University of Technology, P.O. Box 1100, FIN-02015 HUT, Finland

(Received 7 December 1998)

First-principles methods are used to calculate the structures and local vibrational modes of interstitial oxygen pairs in silicon. The staggered  $O_i$ -Si- $O_i$  and skewed  $O_i$ -Si-Si- $O_i$  structures are nearly degenerate in energy. The calculated local vibration frequencies and their pure and mixed  $^{18}\text{O} \rightarrow ^{16}\text{O}$  isotopic shifts agree closely with experiments: the highest frequency is assigned to the skewed and the four lower ones to the staggered structure. This result may clear up the controversy of oxygen dimers in silicon, and also suggests a mechanism for fast oxygen diffusion. [S0031-9007(99)09205-4]

PACS numbers: 61.72.Bb, 63.20.Pw, 78.30.Am

Approximately  $10^{18}$  oxygen atoms/cm<sup>3</sup> appear in as-grown Czochralski silicon, supersaturated and highly inhomogeneously distributed. During subsequent heat treatments oxygen atoms become mobile at temperatures  $>350^\circ\text{C}$  and begin to cluster. Individual oxygen atoms occupying interstitial bond center positions ( $O_i$ ) are known to diffuse by hopping between the neighboring bond center sites with an activation energy of 2.54 eV in a large temperature range of 300–1200 °C [1,2]. However, aggregation of oxygen takes place at a much lower activation energy of about 1.8 eV [3] and oxygen-containing fast diffusing species are needed to explain the aggregation [4,5]. The interstitial oxygen pairs ( $O_{2i}$ ) have been suggested to be a fast diffusing species [4,5]. The local vibration (LV) frequencies of the structures of  $O_{2i}$  can play an important role as fingerprints in clarifying the aggregation mechanisms of oxygen.

When two  $O_i$ 's approach each other their mutual interactions cause splittings in the LV frequencies of  $O_i$  at 1136 and 517  $\text{cm}^{-1}$  [6,7]. Four LV frequencies at 1060, 1012, 690, and 556  $\text{cm}^{-1}$  assigned to the same configuration of  $O_{2i}$  were recently detected and identified experimentally by Hallberg *et al.* [8] and Murin *et al.* [5]. Murin *et al.* [5] also detected an LV frequency at 1105  $\text{cm}^{-1}$  which they associated with another configuration of  $O_{2i}$ . The subsequent study by Öberg *et al.* [9] using the mixed and pure  $^{18}\text{O} \rightarrow ^{16}\text{O}$  isotopes actually proved that the defect giving rise to the four LV frequencies above contains at least two coupled O atoms.

The lowest-energy configuration of  $O_{2i}$  has earlier been assigned to the staggered one [two O atoms having a common Si atom located in the same (110) plane; see Fig. 1] [10]. Recently, Öberg *et al.* [9] reported their finding that a skewed  $O_i$ -Si-Si- $O_i$  configuration [two O atoms separated by two Si atoms located in different (110) planes; see Fig. 2] is, in fact, the ground state. They assigned the four measured LV frequencies (see above) to the LV's of the skewed  $O_i$ -Si-Si- $O_i$  configuration. The purpose of the present Letter is to report LV frequencies for these two configurations of  $O_{2i}$  calculated using

accurate density-functional-theory [11] based methods. The calculations give rise to a new interpretation for the measured LV frequencies and the structure of  $O_{2i}$ . We find that the four measured frequencies originate from the staggered configuration and the frequency at 1105  $\text{cm}^{-1}$  from the skewed  $O_i$ -Si-Si- $O_i$  one. Especially, we find a new local oxygen-induced silicon mode that explains the vanishing of the  $^{18}\text{O} \rightarrow ^{16}\text{O}$  isotopic shift of the lowest measured frequency. This is the first time that *all*

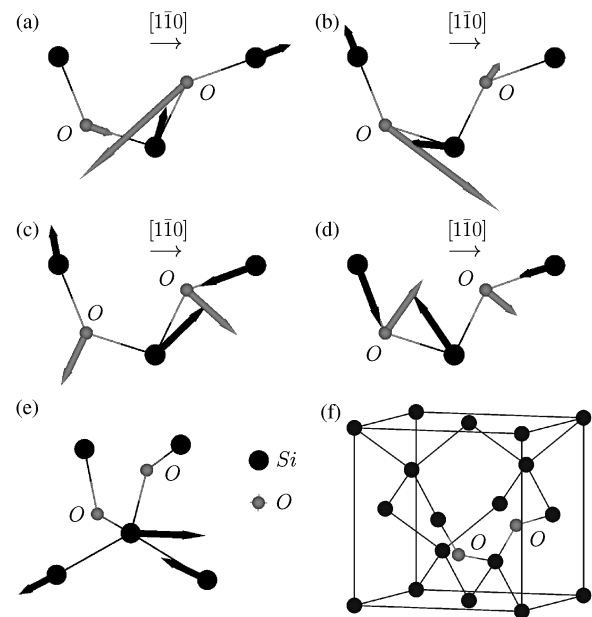


FIG. 1. Calculated vibrational modes for the interstitial oxygen pair in the staggered configuration. Black and grey circles denote silicon and oxygen atoms, respectively. The types and frequencies of the modes are as follows. Asymmetric stretching-type local vibrational modes: (a) 1033  $\text{cm}^{-1}$  and (b) 984  $\text{cm}^{-1}$ ; symmetric stretching-type local vibrational modes: (c) 697  $\text{cm}^{-1}$  and (d) 661  $\text{cm}^{-1}$ ; and (e) oxygen-induced asymmetric silicon vibrational mode: 566  $\text{cm}^{-1}$ . (f) Schematic conventional Si unit cell with two  $O_i$ 's. (a)–(d) are in the (110) plane. (e) is slightly tilted for clarity.

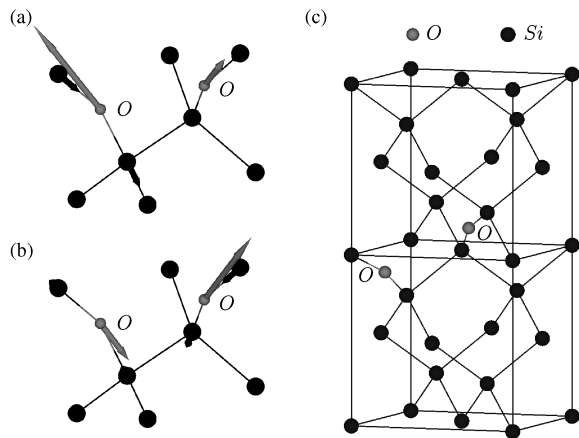


FIG. 2. Calculated asymmetric stretching-type local vibrational modes of the interstitial oxygen pair in the skewed  $O_i$ -Si-Si- $O_i$  configuration: (a)  $1104\text{ cm}^{-1}$  and (b)  $1091\text{ cm}^{-1}$ . (c) Two schematic conventional Si unit cells with two  $O_i$ 's. Black and grey circles denote silicon and oxygen atoms, respectively.

experimental frequencies for  $O_{2i}$  can be explained within one and the same theoretical approach.

The total energy calculations are performed in the local density [12] approximation using a self-consistent plane-wave pseudopotential method. The Perdew-Zunger [13] parametrization of the Ceperley-Alder data [14] is used for the exchange-correlation energy. For silicon we use the norm-conserving Hamann pseudopotential [15]. The pseudopotential is of the fully separable Kleinman-Bylander form [16] and the  $s$  component is used as the local one. For oxygen we use the ultrasoft Vanderbilt pseudopotential [17]. The valence-electron wave functions are expanded in a plane-wave basis set up to a kinetic-energy cutoff of 28 Ry. We use the Monkhorst-Pack  $2^3$   $k$ -point sampling [18] and a 32 atom-site supercell in calculating the LV modes. The total energy is minimized by allowing all ionic coordinates to relax without any constraints until the largest remaining Hellman-Feynman force component is less than  $3\text{ meV}/\text{\AA}$ . The LV calculations are always performed in the zero pressure configuration using the procedure and program by Köhler *et al.* [19]: Every atom is displaced to all six Cartesian directions from the equilibrium position, the electronic structure for this configuration is optimized, and the resulting Hellman-Feynman forces are calculated. The coupling constants for the dynamical matrix are calculated by finite differences using these forces and displacements.

We find that the calculated total energy of the 32 atom-site supercell including the skewed  $O_i$ -Si-Si- $O_i$  configuration is by 0.38 eV below that including the staggered  $O_i$ -Si- $O_i$  configuration. However, improving the accuracy (see Ref. [20]) by increasing the supercell to 128 atom sites and using the  $\Gamma$  point we find that the latter configuration is by 0.1 eV more stable than the former one [21]. Thus, it is important to consider simultaneously the LV's of both configurations when

analyzing the infrared (IR) absorption experiments. This result also suggests a new fast diffusion mechanism for  $O_{2i}$  provided that the diffusion barrier between the two configurations is low enough: Instead of moving both  $O_i$ 's simultaneously as in the model by Ramamoorthy and Pantelides [22] one could move them alternately, first  $O_i^1$  in the skewed  $O_i^1$ -Si-Si- $O_i^2$  configuration to form a staggered  $O_i^1$ -Si- $O_i^2$  configuration and then  $O_i^2$  to form again a transferred skewed  $O_i^1$ -Si-Si- $O_i^2$  configuration [cf. Figs. 2(a) and 1(a)] and so on.

The results from the LV calculations are given in Tables I and II and the relevant LV modes are shown in Figs. 1 and 2.

The calculated LV's in the staggered configuration appear in pairs and bear a clear resemblance to the corresponding LV's of  $O_i$ . The two LV's of the highest frequency pair of  $1033$  and  $984\text{ cm}^{-1}$  [Figs. 1(a) and 1(b)] are of the asymmetric stretching type. In the  $1033$  ( $984$ )  $\text{cm}^{-1}$  LV mode the oxygen atoms vibrate roughly  $180^\circ$  out of phase (in phase). The two LV modes of the next highest frequency pair of  $697$  and  $661\text{ cm}^{-1}$  [Figs. 1(c) and 1(d)] consist analogously of coupled symmetric stretching modes of the two Si- $O_i$ -Si groups. Finally, Fig. 1(e) shows the localized oxygen-induced Si mode of the next highest frequency of  $566\text{ cm}^{-1}$  located just above the region of delocalized vibrations. The Si atom between the two  $O_i$ 's and its two neighboring Si atoms vibrate in an asymmetric stretching mode with much larger amplitudes than the other atoms.

The calculated LV's in the skewed  $O_i$ -Si-Si- $O_i$  configuration also appear in pairs. The LV's of the highest frequency pair of  $1104$  and  $1091\text{ cm}^{-1}$  (Fig. 2) consist of two puckered Si- $O_i$ -Si groups vibrating in asymmetric stretching modes with very different amplitude sizes such that the oxygen atoms vibrate roughly  $180^\circ$  out of phase and in phase, respectively. The two LV's of the next highest frequency pair of  $643$  and  $627\text{ cm}^{-1}$  consist analogously of two puckered Si- $O_i$ -Si groups vibrating in symmetric stretching modes. The mode of the next highest frequency of  $558\text{ cm}^{-1}$  is again an oxygen-induced Si mode consisting mainly of the large vibrations of the two Si atoms between the two  $O_i$ 's and their neighboring Si atoms.

We compare first the upper (asymmetric stretching-type) LV pairs. The calculated LV frequencies for the staggered configuration agree more closely with the experiments than do those for the skewed  $O_i$ -Si-Si- $O_i$  configuration (within 30 and  $80\text{ cm}^{-1}$ , respectively, Table I). The calculated  $^{18}\text{O} \rightarrow ^{16}\text{O}$  isotopic shifts (all silicon atoms are of the  $^{28}\text{Si}$  isotope in this paper) for the staggered configuration ( $-46$  and  $-42\text{ cm}^{-1}$ ) agree again more closely with the experimental isotopic shifts ( $-48$  and  $-43\text{ cm}^{-1}$ ) than do those for the skewed  $O_i$ -Si-Si- $O_i$  configuration ( $-50$  and  $-50\text{ cm}^{-1}$ ) (Table I). The calculated separation of the asymmetric LV frequency pair for the staggered configuration and the  $^{18}\text{O} \rightarrow ^{16}\text{O}$  isotopic shift of this quantity ( $49$  and  $-4\text{ cm}^{-1}$ ) agree much more closely with the corresponding experimental

TABLE I. Local vibration frequencies ( $\text{cm}^{-1}$ ) of  $\text{O}_{2i}$ . S denotes the staggered configuration and SK the skewed  $\text{O}_i$ -Si-Si- $\text{O}_i$  configuration. The symbol “18-16” denotes a mixed  $^{18}\text{O}_i \rightarrow ^{16}\text{O}_i$ -type  $\text{O}_{2i}$ . All silicon atoms are of the  $^{28}\text{Si}$  isotope. The isotopic shifts are given in parentheses in the sixth and seventh column.

|  | $^{16}\text{O}_{2i}$ (S)     | $^{16}\text{O}_{2i}$ (SK)       | 18-16; 16-18 (S)                                      | 18-16; 16-18 (SK)   | $^{18}\text{O}_{2i}$ (S)                          | $^{18}\text{O}_{2i}$ (SK)                             |
|--|------------------------------|---------------------------------|---|---|---|---|
| This work  | 1033, 984<br>697, 661<br>566 | 1104, 1091<br>643, 627<br>558   | 1032, 942; 993, 978<br>693, 655; 691, 658<br>566; 566 | 1103, 1043; 1094, 1052<br>641, 626; 642, 625<br>558; 558  | 987(-46), 942(-42)<br>686(-11), 653(-8)<br>566(0) | 1054(-50), 1041(-50)<br>640(-3), 624(-3)<br>558(0)    |
| Öberg <i>et al.</i><br>calculations <sup>a</sup> | 1101, 926                    | 1085, 1036<br>637<br>581<br>574 | 1072, 907; 1087, 895                                  | 1082, 991; 1053, 1020<br>634; 627<br>579; 578<br>570; 574 |   | 1038(-47), 988(-47)<br>625(-12)<br>577(-4)<br>569(-5) |
| Experiments <sup>a,b</sup><br>(10 K)             | 1060, 1012<br>690<br>556     | 1105                            | ~1060, 970; 1021, 1004<br>686; 686<br>~556; ~556      |   | 1012(-48), 969(-43)<br>680(-10)<br>556(0)         |   |

<sup>a</sup>Reference [9].

<sup>b</sup>References [5,8].

values (48 and  $-5 \text{ cm}^{-1}$ ) than do those for the skewed  $\text{O}_i$ -Si-Si- $\text{O}_i$  configuration (13 and  $0 \text{ cm}^{-1}$ ) (Table II). Also, the calculated separations [23] of the asymmetric LV frequency pairs for the staggered mixed isotope configurations (90;  $15 \text{ cm}^{-1}$ ) agree much more closely with the corresponding experimental values (90;  $17 \text{ cm}^{-1}$ ) than do those for the skewed  $\text{O}_i$ -Si-Si- $\text{O}_i$  ones (60;  $42 \text{ cm}^{-1}$ ) (Table II). And finally, the calculated shift of the average of the asymmetric LV frequency pair and the change induced by the replacement of  $^{16}\text{O}$  by  $^{18}\text{O}$  to this quantity for the staggered configuration ( $-89.5$  and  $6 \text{ cm}^{-1}$ ) agree much more closely with the corresponding experimental values ( $-100$  and  $6.5 \text{ cm}^{-1}$ ) than do those for the skewed  $\text{O}_i$ -Si-Si- $\text{O}_i$  configuration ( $-0.5$  and  $0 \text{ cm}^{-1}$ ) (Table II). Thus this comparison strongly suggests that the measured IR absorption peaks at 1060 and  $1012 \text{ cm}^{-1}$  are due to the *asymmetric* stretching-type LV's of the *staggered*  $\text{O}_{2i}$  [Figs. 1(a) and 1(b)].

The experimentally detected LV frequency of  $1105 \text{ cm}^{-1}$  belonging to a different configuration [5] than the other four frequencies listed in Table I occurs below the large IR absorption peak of  $\text{O}_i$  at  $1136 \text{ cm}^{-1}$  [6]. It is natural to associate the lower frequency (the calculated value of  $1091 \text{ cm}^{-1}$ ) of the asymmetric stretching

frequency pair of the *skewed*  $\text{O}_i$ -Si-Si- $\text{O}_i$  configuration to the experimental frequency of  $1105 \text{ cm}^{-1}$ . The  $1091 \text{ cm}^{-1}$  frequency lies  $58 \text{ cm}^{-1}$  above the highest frequency of  $1033 \text{ cm}^{-1}$  of the staggered configuration which matches well with the corresponding experimental difference of  $1105 - 1060 = 45 \text{ cm}^{-1}$  (Table I). The upper frequency would then be masked by the IR absorption peak of  $\text{O}_i$  (or might be seen as a weak feature on either flank of the peak).

As to the lower (symmetric stretching-type) LV pairs the calculated upper frequency of the staggered configuration of  $697 \text{ cm}^{-1}$  and its  $^{18}\text{O} \rightarrow ^{16}\text{O}$  isotopic shift of  $-11 \text{ cm}^{-1}$  agree closely with the next experimental frequency of  $690 \text{ cm}^{-1}$  and its  $^{18}\text{O} \rightarrow ^{16}\text{O}$  isotopic shift of  $-10 \text{ cm}^{-1}$  (Table I). Since the corresponding quantities of the skewed  $\text{O}_i$ -Si-Si- $\text{O}_i$  configuration (643 and  $-3 \text{ cm}^{-1}$ ) show a less satisfactory agreement the result strongly suggests that the experimental frequency of  $690 \text{ cm}^{-1}$  is the upper frequency of the *symmetric* stretching LV pair of the *staggered* configuration.

The fourth experimental frequency of  $556 \text{ cm}^{-1}$  has no  $^{18}\text{O} \rightarrow ^{16}\text{O}$  isotopic shift and is characterized as Si related [9]. We find a local *oxygen-induced* Si mode of this type just above the region of delocalized vibrations

TABLE II. Separations and shifts of averages of the asymmetric stretching-type local vibration frequency pairs ( $\text{cm}^{-1}$ ) of  $\text{O}_{2i}$ . The shifts of averages are given in parentheses and are calculated from the calculated values of  $1098$  and  $630 \text{ cm}^{-1}$  of  $^{16}\text{O}_i$  and  $1048$  and  $628 \text{ cm}^{-1}$  of  $^{18}\text{O}_i$  [21]. S denotes the staggered configuration and SK the skewed  $\text{O}_i$ -Si-Si- $\text{O}_i$  configuration. All silicon atoms are of the  $^{28}\text{Si}$  isotope. The symbol “18-16” denotes a mixed  $^{18}\text{O}_i \rightarrow ^{16}\text{O}_i$ -type  $\text{O}_{2i}$ .

|   | $^{16}\text{O}_{2i}$ (S)  | $^{16}\text{O}_{2i}$ (SK) | 18-16; 16-18 (S)    | 18-16; 16-18 (SK) | $^{18}\text{O}_{2i}$ (S) | $^{18}\text{O}_{2i}$ (SK) |
|---|---------------------------|---------------------------|---------------------|-------------------|--------------------------|---------------------------|
| This work                                       | 49(-89.5)                 | 13(-0.5)                  | 90; 15              | 60; 42            | 45(-83.5)                | 13(-0.5)                  |
| Öberg <i>et al.</i><br>calculation <sup>a</sup> | 175                       | 49                        | 165; 192            | 91; 33            |                          | 50                        |
| Experiments (10 K)                              | 48(-100) <sup>a,b,c</sup> |                           | 90; 17 <sup>a</sup> |                   | 43(-93.5) <sup>a,b</sup> |                           |

<sup>a</sup>Reference [9].

<sup>b</sup>Reference [8].

<sup>c</sup>Reference [5].

at  $566\text{ cm}^{-1}$  for the staggered configuration [Table I and Fig. 1(e)]. The facts that this frequency agrees closely with the experimental value and in agreement with the experiment shows no  $^{18}\text{O} \rightarrow ^{16}\text{O}$  isotopic shift (Table I) strongly suggest that this LV mode is seen in the experiment at  $556\text{ cm}^{-1}$ .

The LV frequencies of the symmetric stretching frequency pair of the skewed  $\text{O}_i\text{-Si-Si-O}_i$  configuration have not been detected experimentally (see Table I). The reason for this may be as follows. The  $\text{O}_i$ 's interact in this mode weakly, almost like two independent  $\text{O}_i$ 's [21]. And, since the symmetric stretching vibration of  $\text{O}_i$  has not been detected because either a linear  $\text{Si-O}_i\text{-Si}$  "molecule" is infrared inactive [24] or the amplitude of  $\text{O}_i$  in a puckered case is anyway small [21], it is natural that the symmetric stretching modes of the skewed  $\text{O}_i\text{-Si-Si-O}_i$  configuration are not detected either. The absence of only the lower frequency of the symmetric stretching frequency pair of the staggered configuration (Table I) may be understood in the same way. The  $\text{O}_i$ 's in the lower frequency mode vibrate roughly in phase and interact thus less than the  $\text{O}_i$ 's in the upper frequency mode vibrating roughly  $180^\circ$  out of phase [Figs. 1(d) and 1(c)]. Thus, the symmetric stretching vibrations of the  $\text{O}_i$ 's in the lower frequency mode resemble more those of a single  $\text{O}_i$  which might explain the absence.

Öberg *et al.* [9] using an *H*-terminated cluster of 88 atoms (44 Si atoms) reported that their calculated frequencies for the skewed  $\text{O}_i\text{-Si-Si-O}_i$  configuration correlate quite well with the four experimental frequencies while those for their configuration (i)—corresponding to the staggered geometry—do not (Table I). Especially the large mixed  $^{18}\text{O} \rightarrow ^{16}\text{O}$  isotopic shifts in the frequencies of  $1101$  and  $926\text{ cm}^{-1}$ —reflecting an excessive interaction between the oxygen atoms—ruled out their configuration (i) (Table I). Also the large separation of  $175\text{ cm}^{-1}$  found for the asymmetric stretching pair (Table II) reflects a large interaction. These results differ considerably from ours and more work is needed to resolve these discrepancies.

In conclusion, we find from accurate total energy pseudopotential calculations that the experimental LV frequencies of  $1060$ ,  $1012$ ,  $690$ , and  $556\text{ cm}^{-1}$  are the upper and lower frequencies of the asymmetric stretching-type frequency pair, the upper frequency of the symmetric stretching-type frequency pair, and the frequency of the oxygen-induced silicon mode of the staggered  $\text{O}_{2i}$  defect, respectively. The  $1105\text{ cm}^{-1}$  frequency is assigned to the lower frequency of the asymmetric stretching-type frequency pair of the skewed  $\text{O}_i\text{-Si-Si-O}_i$  configuration of  $\text{O}_{2i}$ .

The authors wish to thank Dr. T. Mattila for many valuable discussions. This work has been supported by the Academy of Finland. We acknowledge the generous computing resources of the Center for the Scientific

Computing (CSC), Espoo, Finland. M. P. acknowledges the financial support of the Väisälä Foundation.

- 
- [1] J. W. Corbett, R. S. McDonald, and G. D. Watkins, *J. Phys. Chem. Solids* **25**, 873 (1964).
  - [2] J. C. Mikkelsen, *Mater. Res. Soc. Symp. Proc.* **59**, 19 (1986).
  - [3] P. Wagner, J. Hage, J. M. Trombetta, and G. D. Watkins, *Mater. Sci. Forum* **83–87**, 401 (1992).
  - [4] R. C. Newman, in *Early Stages of Oxygen Precipitation in Silicon*, edited by R. Jones (Kluwer Academic Publishers, Dordrecht, 1996), p. 19.
  - [5] L. I. Murin, T. Hallberg, V. P. Markevich, and J. L. Lindström, *Phys. Rev. Lett.* **80**, 93 (1998).
  - [6] H. J. Hrostowski and B. J. Alder, *J. Chem. Phys.* **33**, 980 (1960).
  - [7] D. R. Bosomworth, W. Hayes, A. R. L. Spray, and G. D. Watkins, *Proc. R. Soc. London A* **317**, 133 (1970).
  - [8] T. Hallberg, J. L. Lindström, L. I. Murin, and V. P. Markevich, *Mater. Sci. Forum* **258–263**, 361 (1997).
  - [9] S. Öberg, C. P. Ewels, R. Jones, T. Hallberg, J. L. Lindström, L. I. Murin, and P. R. Briddon, *Phys. Rev. Lett.* **81**, 2930 (1998).
  - [10] M. Needels, J. D. Joannopoulos, Y. Bar-Yam, and S. T. Pantelides, *Phys. Rev. B* **43**, 4208 (1991).
  - [11] P. Hohenberg and W. Kohn, *Phys. Rev.* **136**, B864 (1964).
  - [12] W. Kohn and L. J. Sham, *Phys. Rev.* **140**, A1133 (1965).
  - [13] J. Perdew and A. Zunger, *Phys. Rev. B* **23**, 5048 (1981).
  - [14] D. M. Ceperley and B. J. Alder, *Phys. Rev. Lett.* **45**, 566 (1980).
  - [15] D. H. Hamann, *Phys. Rev. B* **40**, 2980 (1989).
  - [16] L. Kleinman and D. M. Bylander, *Phys. Rev. Lett.* **48**, 1425 (1982).
  - [17] D. Vanderbilt, *Phys. Rev. B* **41**, 7892 (1990); K. Laasonen, A. Pasquarello, R. Car, C. Lee, and D. Vanderbilt, *Phys. Rev. B* **47**, 10 142 (1993).
  - [18] H. J. Monkhorst and J. D. Pack, *Phys. Rev. B* **13**, 5188 (1976).
  - [19] Th. Köhler, Th. Frauenheim, and G. Jungnickel, *Phys. Rev. B* **52**, 11 837 (1995).
  - [20] M. Pesola, J. von Boehm, S. Pöykkö, and R. M. Nieminen, *Phys. Rev. B* **58**, 1106 (1998); M. J. Puska, S. Pöykkö, M. Pesola, and R. M. Nieminen, *Phys. Rev. B* **58**, 1318 (1998).
  - [21] M. Pesola, J. von Boehm, T. Mattila, and R. M. Nieminen (to be published).
  - [22] M. Ramamoorthy and S. T. Pantelides, *Solid State Commun.* **106**, 243 (1998).
  - [23] In the 18-16 case the heavier  $^{18}\text{O}$  is to the left in Fig. 1, has a large amplitude in the lower frequency mode [Fig. 1(b)], and causes an increase in the separation from  $49$  to  $90\text{ cm}^{-1}$ . In the 16-18 case  $^{18}\text{O}$  is to the right in Fig. 1, has a large amplitude in the upper frequency mode [Fig. 1(a)], and causes a decrease in the separation from  $49$  to  $15\text{ cm}^{-1}$ .
  - [24] E. Artacho, A. Lizón-Nordström, and F. Ynduráin, *Phys. Rev. B* **51**, 7862 (1995).